

Original Full Length Article

Differentially circulating miRNAs after recent osteoporotic fractures can influence osteogenic differentiation



Sylvia Weilner^a, Susanna Skalicky^b, Benjamin Salzer^a, Verena Keider^a, Michael Wagner^b, Florian Hildner^d, Christian Gabriel^d, Peter Dovjak^e, Peter Pietschmann^f, Regina Grillari-Voglauer^c, Johannes Grillari^{a,b,c,*}, Matthias Hackl^{a,b}

^a CD Laboratory on Biotechnology of Skin Aging, Department of Biotechnology, BOKU – University of Natural Resources and Life Sciences Vienna, 1190 Vienna, Austria

^b TAmiRNA GmbH, 1190 Vienna, Austria

^c Evercyte GmbH, 1190 Vienna, Austria

^d Red Cross Blood Transfusion Service of Upper Austria, Austrian Cluster for Tissue Regeneration, 4020 Linz, Austria

^e Salzkammergut-Klinikum Gmunden, 4810 Gmunden, Austria

^f Department of Pathophysiology and Allergy Research, Center for Pathophysiology, Infectiology and Immunology, Medical University Vienna, 1090 Vienna, Austria

ARTICLE INFO

Article history:

Received 14 December 2014

Revised 8 May 2015

Accepted 21 May 2015

Available online 28 May 2015

Edited by Mark Cooper

Keywords:

Osteoporosis

Circulating microRNA (miRNA)

Bone

Quantitative PCR (qPCR)

Osteogenic differentiation

Mesenchymal stem cells

ABSTRACT

Osteoporosis is the consequence of altered bone metabolism resulting in the systemic reduction of bone strength and increased risk of fragility fractures. MicroRNAs (miRNAs) regulate gene expression on a post-transcriptional level and are known to take part in the control of bone formation and bone resorption. In addition, it is known that miRNAs are secreted by many cell types and can transfer “messages” to recipient cells. Thus, circulating miRNAs might not only be useful as surrogate biomarkers for the diagnosis or prognosis of pathological conditions, but could be actively modulating tissue physiology.

Therefore, the aim of this study was to test whether circulating miRNAs that exhibit changes in recent osteoporotic fracture patients could be causally related to bone metabolism.

In the first step we performed an explorative analysis of 175 miRNAs in serum samples obtained from 7 female patients with recent osteoporotic fractures at the femoral neck, and 7 age-matched female controls. Unsupervised cluster analysis revealed a high discriminatory power of the top 10 circulating miRNAs for patients with recent osteoporotic fractures. In total 6 miRNAs, miR-10a-5p, miR-10b-5p, miR-133b, miR-22-3p, miR-328-3p, and let-7g-5p exhibited significantly different serum levels in response to fracture (adjusted p-value < 0.05). These miRNAs were subsequently analyzed in a validation cohort of 23 patients (11 control, 12 fracture), which confirmed significant regulation for miR-22-3p, miR-328-3p, and let-7g-5p. A set of these and of other miRNAs known to change in the context of osteoporotic fractures were subsequently tested for their effects on osteogenic differentiation of human mesenchymal stem cells (MSCs) *in vitro*. The results show that 5 out of 7 tested miRNAs can modulate osteogenic differentiation of MSCs *in vitro*.

Overall, these data suggest that levels of specific circulating miRNAs change in the context of recent osteoporotic fractures and that such perturbations of “normal” levels might affect bone metabolism or bone healing processes.

© 2015 The Authors. Published by Elsevier Inc. This is an open access article under the CC BY-NC-ND license (<http://creativecommons.org/licenses/by-nc-nd/4.0/>).

Introduction

Osteoporotic fractures are caused by decreased bone strength, which can occur due to low bone mass and microarchitectural changes in bone tissue [1]. Such fractures are the critical hard outcome of osteoporosis, a disease that affects more than 75 million people in the United States, Europe and Japan. With a lifetime fracture risk of 30%–40% (vertebral

or non-vertebral fractures), osteoporosis has an incidence rate similar to that of coronary heart disease. Furthermore, with the exception of forearm fractures, osteoporotic fractures are associated with increased mortality. Most fractures cause acute pain and lead to patient hospitalization, immobilization and often slow recovery [2–4].

Recently, increased attention has been attributed to the importance of microRNAs (miRNAs), small non-coding RNAs that regulate gene expression [5], in the context of bone formation [6,7] as well as bone disease [8]. For example, several miRNAs were shown to silence osteogenic inhibitors during stem cell differentiation into osteocytes [9], to mediate BMP-2 dependent osteoblast proliferation and differentiation [10], or contribute to the regulation of WNT-signaling [11]. *In vivo*, the

* Corresponding author at: Department of Biotechnology, BOKU, University of Natural Resources and Life Sciences Vienna, Muthgasse 18, 1190 Vienna, Austria.

E-mail addresses: johannes.grillari@boku.ac.at (J. Grillari), matthias.hackl@tamirma.com (M. Hackl).

relevance of miRNA for bone remodeling was shown in studies of mice with conditional knockout of Dicer in osteoclasts, which results in the ablation of mature miRNA production in these cells. Compared to control strains, these mice exhibited significantly decreased number of osteoclasts and therefore bone resorption [12]. In addition, circulating miRNAs have been identified as biomarkers for a variety of diseases, including age-associated diseases [13]. In particular, a series of very recent publications has identified differences in tissue and circulating miRNAs in the serum of aged individuals [14] as well as fracture patients with low versus normal bone mineral density [15] or altered BMD levels without fractures [16].

Data exist, which show that circulating miRNAs can be taken up by cells and thereby influence the recipient cell's behavior in the context of diverse biological functions [17,18]. Therefore, based on the importance of miRNAs for bone homeostasis and their extracellular shuttling, we hypothesized that circulating miRNAs have the potential to be not only surrogate biomarkers (byproducts) of bone metabolism, but actually markers with functional relevance to osteogenic and/or osteoclast differentiation. As a consequence such circulating miRNAs might find future applications as therapeutic targets in order to influence bone metabolism, similar to recently established drug targets derived from important signaling pathways such as WNT or RANKL [19,20].

In order to explore this hypothesis, we first quantified the levels of 175 circulating miRNAs in serum samples from post-menopausal women with recent femoral-neck fractures, validated the most promising candidates in an independent validation cohort, and selected a set of the here identified as well as previously published circulating miRNAs for functional characterization in the context osteogenic differentiation of mesenchymal stem cells *in vitro*.

Materials and methods

Study population

Ethical approval for the analysis of human samples according to the Declaration of Helsinki was granted by the Upper Austrian ethics committee, and informed consent was obtained from all participants in this study. Serum samples were obtained from 37 female post-menopausal subjects, of which 19 had recently sustained osteoporotic fractures at the femoral neck (ICD Codes S72.0 and S72.1). Osteoporotic fractures were defined by being caused by low-impact trauma and patients' age > 65 years. All subjects were of white Caucasian descent and were not undergoing chronic treatment with substances known to affect bone metabolism such as anti-resorptive or bone anabolic drugs or glucocorticoids. Patients with pathologic fractures were excluded. High-trauma fractures were excluded similar to pathologic fractures — defined as fractures due to local tumors or tumor-like lesions. Blood samples were drawn between 8:00 am and 10:00 am and routinely tested for 25-OH Vitamin D₃, and parathyroid hormone (PTH). Bone mineral density (BMD) by DXA scans at the femoral neck and calculated T-scores were only available for half of the patients, and therefore not included in the analysis.

Cell culture

Subculturing

Subcutaneous adipose tissue was obtained under written consent from patients during tumescence liposuction under local anesthesia at the Red Cross Upper Austria. ASCs were isolated from 2 donors as described before [21], termed HUF803 and HUF851, and cultivated in DMEM-low glucose/HAM's F-12 (GE-Healthcare) supplemented with 4 mM L-glutamine, 10% fetal calf serum (FCS, Sigma) and 1 ng/mL recombinant human basic fibroblast growth factor (rhFGF, R&D Systems) at 37 °C, 5% CO₂ and 95% air humidity. Cells were passaged once or twice a week at a split ratio of 1:4.

MicroRNA transfection

ASCs were transfected by electroporation using the Neon Transfection System (Life Technologies) according to the manufacturer's instruction. Briefly 100,000 ASCs were mixed with 10 µL buffer and 1 µL of 10 µM miRNA. Subsequently electroporation (1400 V, 10 ms pulse width and 3 pulses) was performed. Three days after transfection, differentiation was started.

Osteogenic differentiation

For osteogenic differentiation transfected ASCs were seeded at a density of 2×10^3 cell per well. 72 h after seeding cell growth medium of ASCs was aspirated and cells were cultivated in osteogenesis induction medium DMEM-low glucose (GE-Healthcare), 10% FCS (Sigma), 4 mM L-glutamine, 10 nM dexamethasone, 150 µM ascorbate-2-phosphate, 10 mM β-glycerol phosphate and 10 nM vitamin-D3.

Alkaline phosphatase assay (ALP assay)

Quantification of alkaline phosphatase activity was performed using 2 different donors of ASCs and 3 independent replicate wells each. In order to quantify the activity of alkaline phosphatase, osteogenesis medium was aspirated and cells were lysed in 100 µL ALP lysis buffer (0.25% v/v Triton X-100 in 0.5 M 2-amino-2-methyl-1-propanol (Sigma-Aldrich), 2.0 mM magnesium chloride (VWR)) 7 days after induction of osteogenesis. Subsequently the cell lysate was centrifuged for 10 min at 13,000 ×g and 50 µL ALP Buffer A (0.5 M 2-amino-2-methyl-1-propanol (Sigma-Aldrich)), 2.0 mM magnesium chloride (VWR), and p-nitrophenylphosphate disodium hexahydrate (Sigma-Aldrich) were added to the supernatant per sample before it was incubated for 20 min at room temperature. Finally 50 µL 0.2 M NaOH was added to stop the reaction and absorption was measured at 405 nm relative to 620 nm.

Alizarin staining

Quantification of calcium deposition by Alizarin staining was performed using 2 ASC donors and 8 replicate wells each. Cells were fixed for 1 h in 70% ethanol at −20 °C. After rinsing, cells were stained for 20 min with 40 mM Alizarin Red solution (Sigma). Subsequently cells were washed with PBS until all traces of unbound dye were removed. For quantification Alizarin was extracted for 30 min using 200 µL 0.1 M HCL/0.5% SDS solution. The extracted dye was quantified at 425 nm.

RNA isolation

Serum samples were collected by centrifugation at room temperature at 2000 ×g for 15 min after incubation at room temperature for 30 min, and frozen at −80 °C for long term storage. Upon RNA isolation, serum was thawed at 37 °C, centrifuged at 12,000 ×g for 5 min and 200 µL serum was homogenized in 750 µL Qiazol containing 35 fmol synthetic cel-miR-39-3p spike-in control. RNA isolation was performed using chloroform extraction and ethanol precipitation following by purification using the miRNeasy isolation kit (Qiagen, Germany) with the following modifications from the standard protocol: 200 µL plasma was homogenized in 750 µL Qiazol. Exactly 500 µL aqueous phase was taken and glycogen (Ambion, TX) was added to a final concentration of 50 µg/mL and precipitated with 750 µL 100% ethanol. Columns were washed three times with RPE buffer and plasma-RNA was eluted once in 30 µL nuclease-free water and stored at −80 °C. Quantitation of cel-miR-39-3p by quantitative PCR was performed to ensure equal purification efficiencies for all samples (Supporting Fig. 1A), and hemolysis was identified using a difference between miR-23a and miR-451a of 7 as cut-off [22].

RNA isolation from cells was performed by Trizol/chloroform extraction and isopropanol precipitation using glycogen as a carrier at 1 µg/µL (Thermo Scientific). RNA pellets were washed twice with 70% EtOH, air-dried and resuspended in 50 µL of nuclease-free water. RNA concentration was analyzed photometrically at 260 nm as well as purity at 260/280 nm and 260/230 nm using a NanoDrop (Thermo Fisher).

microRNA qPCR analysis from cellular total RNA

Two microliters of total RNA was diluted to 5 ng/μL and reverse transcribed using the Universal cDNA Synthesis Kit II together with UniSp6 spike-in control to monitor the presence of enzyme inhibitors. Real-time qPCR reactions were performed in 10 μL reaction volumes in triplicates using SYBR Green Mix (Exiqon, Denmark) and commercially available LNA-enhanced miRNA primer assays (Exiqon, Denmark) and assays for U6 and 5S rRNA as reference RNAs, respectively. PCR conditions were 95 °C for 10 min, 45 cycles of denaturation (95 °C, 10 s) and annealing/elongation (60 °C, 60 s), and melting curve analysis on an LC 480 (Roche). Cp-values were calculated using the 2nd derivative method and ddCt analysis was performed to calculate log₂-fold differences between control- and miRNA-transfected samples.

microRNA qPCR analysis from serum total RNA

Real-time quantitative PCR (RT-qPCR) analysis of circulating microRNAs was performed as previously reported [23]. In brief, screening of miRNA expression was conducted using 384-well serum/plasma focus panels (Cat# 203842, Exiqon, Denmark), which cover 175 distinct human miRNAs that have been repeatedly found to circulate in serum or plasma. First, 4 μL of isolated RNA was reverse transcribed in 20 μL reactions using the miRCURY LNA Universal RT reaction kit. UniSp3 and UniSp6 are synthetic controls that were added at this step and subsequently analyzed to detect presence of enzyme inhibitors (Supporting Fig. 1B). RT-reactions were diluted 50-fold prior to qPCR analysis and each miRNA was assayed once per sample in a 10 μL reaction using the Roche LC 480 Real-Time PCR System (Roche, Germany).

qPCR data analysis

Melting curve analysis was performed and miRNA PCR reactions with more than one peak were excluded from the analysis. Amplification efficiencies were calculated using algorithms similar to the linreg software package. Efficiencies ranged between 1.8 and 2.1 for most miRNAs. Individual reactions that gave efficiencies < 1.6 were excluded from the data set. Background levels for each miRNA were generated by assaying a “no template” cDNA synthesis control on a full serum/plasma focus panel plate. The majority of miRNA assays did not yield any signal and background Cp was set to 42. We required every miRNA assay to exhibit signals > 5 Cps lower than the background value to be included in the analysis. Normalization of Cp-values was performed based on the average Cp of the miRNA assays detected across all 14 samples (114 samples). Normfinder software was used to confirm that the stability of the average Cp was higher than the stability of any individual miRNA assay in the data set [24]. The following equation was used for normalization: normalized Cp (dCp) = average Cp (114 assays) – assay Cp (sample). This results in a delta Cp (dCp) value, which is a relative log₂-transformed measure for expression where higher values indicate a higher concentration and lower dCp values indicate lower concentration in plasma. All relevant raw and normalized data have been submitted to NCBI's gene expression omnibus under the guidelines for minimal information about qPCR experiments [25], and can be accessed under the number GSE60230.

Statistical analysis

Quantitative PCR data

Hierarchical clustering using Euclidean distance and complete linkage was performed in R using the “heatmap.2” function of the ggplot2 package. For the analysis of differentially regulated circulating miRNAs normal distribution was confirmed using Shapiro–Wilk test in GraphPad Prism 5.0. Subsequently, two-sided t-tests were performed and p-values were adjusted for multiple testing using Benjamini–Hochberg's method for false-discovery rate calculation.

Markers of osteogenic differentiation

Statistical analysis of ALP and Alizarin quantitation between miRNA transfected and control samples was determined using the Holm–Sidak method, with alpha = 5.000%. Each comparison was analyzed individually, without assuming a consistent SD.

Results

Donor and sample characteristics

In order to discover changes in circulating miRNA levels in post-menopausal women suffering from low-trauma fractures at the femoral neck, 37 serum donors were recruited (Table 1), 19 of which were obtained from patients with recent fractures. The majority of subjects were free of co-morbidities (21 subject, 56.8%), while 7 subjects (4 controls, 3 fracture, 18.9% total) were diagnosed with type-2 diabetes, which was the most frequently observed co-morbidity.

Serum samples were taken within 14 days after surgery. During the discovery phase 14 samples (7 fracture, 7 controls) could be analyzed. For this purpose, post-menopausal women were selected with similar distribution of age, vitamin D, and PTH. Differences were observed for BMD at the femoral neck (not significant) and body mass index (BMI, significant). The validation set consisted of 23 female post-menopausal samples (12 fracture, 11 controls) with similar distribution of age, BMI, vitamin D, and PTH levels between the control and fracture group. However, compared to the discovery group, age was significantly higher in the validation group (Table 1).

Discovery sample analysis

For the discovery study sample and RNA quality were checked at several stages during the analysis process. Cel-miR-39-3p was spiked prior to RNA isolation and analyzed by qPCR to ensure consistent RNA isolation (Supporting Fig. 1a). In addition, two synthetic spike-in controls, UniSp3 and UniSp6, were added to the isolated RNA in order to test for the presence of enzyme inhibitors (Supporting Fig. 1b). The uniform Cp values obtained for all spike-ins confirmed successful RNA isolation, reverse transcription and qPCR. Based on a recent study by Blondal et al., the degree of contamination with erythrocyte RNA was assessed by computing a hemolysis index (difference between miR-23a-3p and miR-451a-5p), which is known to be highly present in erythrocytes [22]. The results indicated relatively strong hemolysis (index = 7) in five samples (Supporting Fig. 1c). Therefore we set out to identify those miRNAs that are most affected by hemolysis by correlating Cp-values to the hemolysis index across all 14 samples (Supporting Fig. 2) using Pearson correlation. In total 10 miRNAs with a Pearson correlation coefficient (PCC) > 0.9 (including miR-451a) were identified and removed from the data set. Thus, a total of 165 miRNAs remained in the data-set.

Distribution of missing signals indicates no complete gain/loss of circulating miRNAs in fracture patients

Out of 165 miRNAs, 114 (69%) gave valid signals (above background) in all 14 samples (Supporting Fig. 3a). In cases where signals were found to be below background it cannot be discerned if this failure to detect specific miRNAs (“NA-values”) is due to very low serum concentration, which would be of biological relevance, or if it is due to technical reasons. Therefore, the number and distribution of NA-values were analyzed in detail: out of 165 features, 10 gave valid signals in less than 7 (<50%) of samples, which were removed from further analyses since no differences in distribution between fracture and control samples were observed (Supporting Fig. 3a). The remaining 41 features, which gave valid signals in ≥50% of samples, but showed at least one missing value were analyzed in detail for their distribution of valid values (Supporting Fig. 3b). Two miRNAs, hsa-miR-1 and hsa-miR-154,

Table 1
Descriptive data of study participants.

	Discovery				Validation			
	Control	SEM	Fracture	SEM	Control	SEM	Fracture	SEM
Number of samples	7	–	7	–	11	–	12	–
Age (years)	71.0	±2.3	72.4	±3.2	81.5	±1.5	77.8	±1.4
BMI (kg/m ²) ^a	29.6	±1.3	23.35	±1.3	24.4	±0.9	23.9	±1.3
Vitamin D (µg/L)	20.1	±4.2	15.0	±2.4	18.4	±3.3	19.0	±3.9
PTH (ng/L)	42.4	±3.9	55.2	±15.7	63.9	±7.2	46.3	±6.1
Time between surgery and sampling (days)	–	–	11.3	±1.2	–	–	14.0	±1.6

Data are expressed as mean.

Control = study participants who have not sustained femoral fractures.

Fracture = study participants who have sustained femoral fractures and undergone surgery.

^a p-Value < 0.05, discovery study.

showed differences of more than 30% in the number of valid signals. However, the present values for both miRNAs showed no differences between fracture and control samples.

Altogether, 155 miRNAs that gave valid signals in more than 50% of the samples were subject to statistical data analysis.

Biostatistical analysis identifies 6 differentially expressed circulating miRNAs in patients with femoral neck fractures

Differential expression analysis was performed based on global-mean normalized delta-Cp values to identify circulating miRNAs that are deregulated in serum upon the recent occurrence of femoral neck fractures in post-menopausal women. Therefore, normal distribution of dCp-values was confirmed by Shapiro–Wilkinson test, and subsequently Student's t-test was performed using multiple testing corrections of p-values according to Benjamini–Hochberg (control of false-discovery rate, FDR). The number of up- and down-regulated miRNAs between fracture and control samples was generally balanced with a total of 6 miRNAs that exhibited significant regulation based on the adjusted p-value cut-off 0.05 (Fig. 1a): three up-regulated miRNAs (miR-10a-5p, miR-10b-5p, miR-22-3p) and three down-regulated miRNAs (miR-133b, miR-328-3p, let-7g-5p). All 155 miRNAs were ranked according to their adjusted p-value and using an initial FDR-threshold of 0.2, twenty-one miRNAs were identified (Table 2), with a potential of 4 false-positive miRNAs (i.e., 20% out of 21 miRNAs).

In order to assess the discriminatory power by unsupervised clustering, dCp values of the top-10 regulated miRNAs with an FDR below 0.1 (less than 1 false-positive miRNA), were used for heatmap analysis and hierarchical clustering based on the Euclidean distance metric (Fig. 1b). The results indicate that together, the top-10 regulated miRNAs are sufficient for 100% correct classification of fracture and control samples, as can be seen by the sample dendrogram in Fig. 1b.

Validation of differentially present miRNAs in an independent cohort

In order to validate the results obtained from the discovery study, a validation cohort comprising 23 samples (Table 1) was analyzed using specific primers for the 6 differentially regulated miRNAs. In addition, sample and data quality control was performed similarly to the discovery data set using spike-in and endogenous controls (Supplemental Fig. 4), which confirmed successful RNA isolation and cDNA synthesis as well as absence of hemolysis for all samples.

Figs. 2(a–f) present the data obtained for the additional fracture patients (n = 12) compared to control patients (n = 11) analyzed by parametric student's t-tests: the previously observed regulation of miR-10a/b-5p and miR-133b could not be confirmed, while fold changes for miR-22-3p, miR-328-3p and let-7g-5p reached significance. In the case of miR-22-3p, which was found to be moderately up-regulated in the discovery cohort, significant down-regulation by more than 70% was observed in the validation cohort.

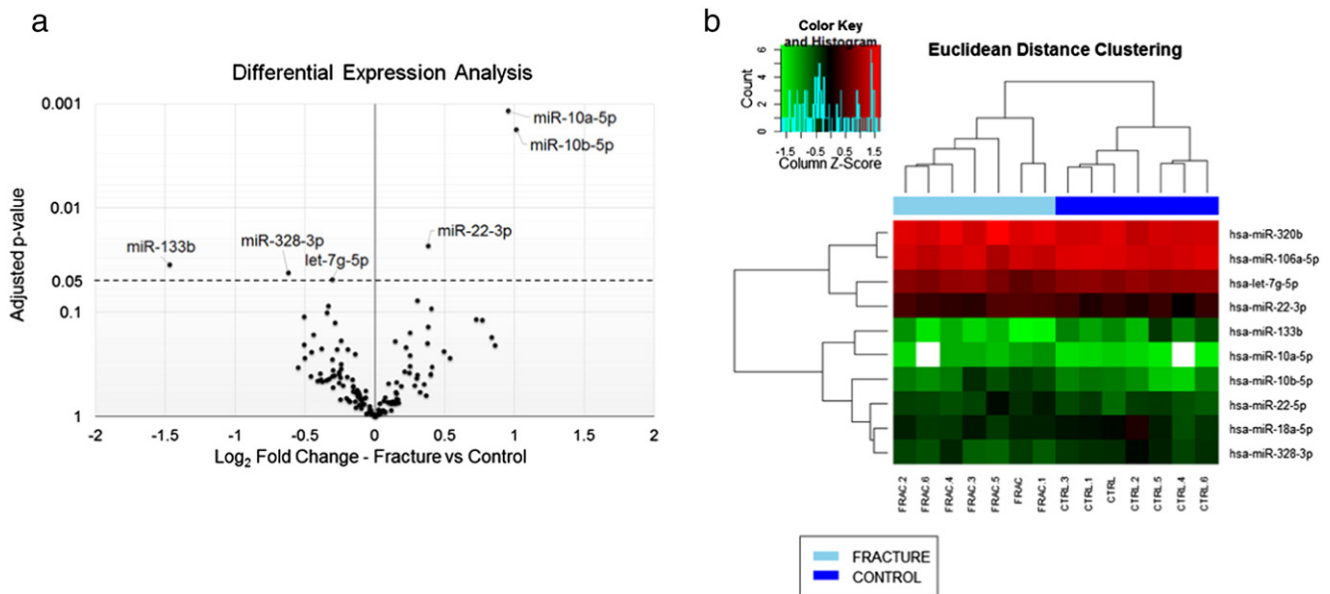


Fig. 1. Differential expression analysis of circulating miRNAs. (a) Volcano plot depicting the log₂ fold change (fracture vs control) against the adjusted p-value of all 155 analyzed miRNAs. The adjusted p-value threshold of 0.05 is indicated as a dotted line, and all significantly regulated miRNAs are labeled with their names. (b) Heatmap depicting the expression of the top-10 miRNAs (sorted according to adjusted p-values) across all 14 samples. Hierarchical clustering was performed using Euclidean distance and complete linkage.

Table 2

Discovery study – list of miRNAs with altered levels between fracture and control patients (top 20 miRNAs sorted by adj. p-value).

Rank	miRNA ID	Presence call	Fracture		Control		Effect size		Statistics	
			Mean dCp	SD dCp	Mean dCp	SD dCp	log ₂ FC (ddCp)	Linear FC	Two-sided parametric t-test p-value	BH adjusted p-value (FDR)
1	hsa-miR-10a-5p	12	-4.10	0.40	-5.05	0.25	0.952	1.935	0.001	0.0012
2	hsa-miR-10b-5p	14	-2.51	0.41	-3.52	0.41	1.012	2.017	0.001	0.0017
3	hsa-miR-22-3p	14	0.19	0.28	-0.18	0.18	0.376	1.298	0.017	0.0228
4	hsa-miR-133b	14	-4.63	1.04	-3.16	1.00	-1.472	0.360	0.028	0.0344
5	hsa-miR-328-3p	14	-2.30	0.53	-1.68	0.37	-0.625	0.649	0.034	0.0412
6	hsa-let-7g-5p	14	1.25	0.27	1.55	0.19	-0.309	0.807	0.041	0.0480
7	hsa-miR-320b	14	3.03	0.34	2.73	0.14	0.301	1.232	0.067	0.0771
8	hsa-miR-106a-5p	14	2.54	0.37	2.88	0.21	-0.334	0.794	0.078	0.0861
9	hsa-miR-22-5p	14	-1.84	0.25	-2.24	0.46	0.402	1.321	0.086	0.0915
10	hsa-miR-18a-5p	14	-1.67	0.25	-1.32	0.39	-0.344	0.788	0.092	0.1007
11	hsa-miR-143-3p	14	-0.18	0.49	0.33	0.50	-0.509	0.703	0.101	0.1092
12	hsa-miR-30a-5p	13	-3.81	0.54	-4.54	0.79	0.723	1.651	0.109	0.1160
13	hsa-miR-376a-3p	14	-2.44	0.70	-3.21	0.86	0.766	1.701	0.116	0.1171
14	hsa-miR-17-5p	14	-1.20	0.31	-0.91	0.28	-0.289	0.819	0.117	0.1255
15	hsa-miR-103a-2-5p	12	-4.53	0.29	-4.91	0.40	0.381	1.302	0.129	0.1372
16	hsa-miR-320a	14	3.06	0.37	2.81	0.14	0.249	1.189	0.148	0.1571
17	hsa-miR-324-5p	14	-2.57	0.66	-2.13	0.28	-0.442	0.736	0.157	0.1634
18	hsa-miR-127-3p	14	-3.26	0.98	-4.10	0.97	0.835	1.783	0.163	0.1725
19	hsa-miR-18b-5p	14	-0.85	0.32	-0.61	0.27	-0.244	0.844	0.177	0.1859
20	hsa-miR-21-5p	14	5.04	0.23	4.90	0.10	0.145	1.106	0.186	0.1890
21	hsa-miR-378	14	-1.02	0.41	-1.39	0.51	0.372	1.294	0.189	0.1980

Cp, cycle threshold from qPCR; dCp, delta-Cp = global mean normalized Cp value.

ddCp, delta-delta-Cp value = difference in normalized dCp values between both groups.

BH, Benjamini-Hochberg, FDR, false discovery rate; SD, standard deviation.

Screening of microRNA function using an *in vitro* assay for osteogenic differentiation

As a next step we not only compared the here identified differentially circulating miRNAs from discovery and validation experiments with published work describing functions for these miRNAs in relation to bone metabolism, but also compared them to the 2 so far published examples of circulating miRNAs in the context of osteoporosis [15,16]

(Table 3). Importantly, the design of both published studies was different from the design of the here presented study: Seeliger et al. [15] profiled serum levels of a total of 83 miRNAs in subjects with osteoporotic fracture (BMD T-score < -2.5) to fractured non-osteoporotic subjects (BMD T-score > 1.0). This allows correlation of circulating miRNA levels to manifest osteoporosis (i.e., with fractures) while it does not allow the assessment that recent fractures have on circulating miRNA levels. On the other hand, Li et al. [16] correlate the levels of three pre-

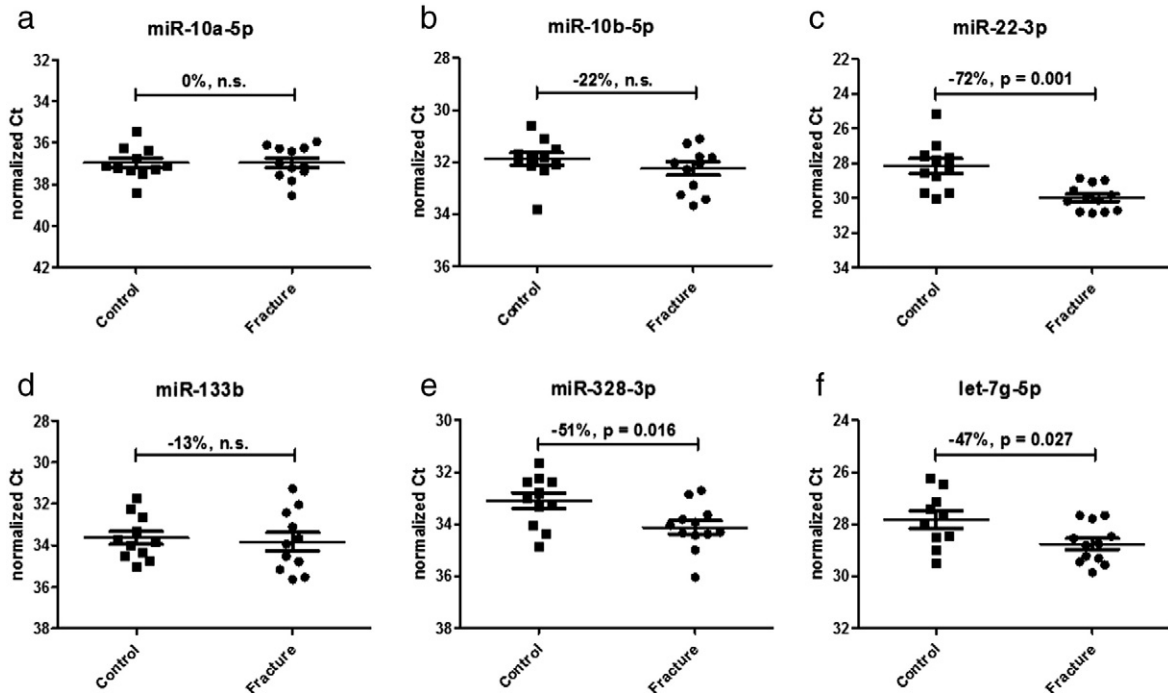


Fig. 2. miRNA validation in an independent sample subset. (a–f) Scatterplots depicting the normalized Cp-values of selected miRNAs in the validation cohort consisting of 11 controls and 12 fracture samples. Y-axis labels presenting normalized Cp-values were inverted in order to allow intuitive interpretation of up- and down-regulation. Lines overlapping the data points depict mean and SEM values. Percent fold change in the fracture group is given together with p-values calculated from parametric student's t-test analysis. n.s. (not significant) indicates p-values > 0.05.

Table 3
Circulating microRNAs in osteoporosis and osteoporotic fractures.

miRNA ID	Original source	Experimental setting	Observed effect	Published main effects in the context of bone metabolism in vitro	References	Selected miRNAs
let-7g-5p	This study	Low trauma fracture vs control	Down-regulated	Promotes osteogenic differentiation	Wei, et al. [27]	✓
miR-100-5p	Seeliger et al.	Osteoporotic Fx vs non-osteoporotic Fx	Up-regulated	Inhibits osteogenic differentiation	Zeng, et al. [28]	✓
miR-10b-5p	This study	Low trauma fracture vs control	Up-regulated ^a	Is up-regulated during osteogenic differentiation	Trompeter, et al. [9]	✓
miR-122a	Seeliger et al.	Osteoporotic Fx vs non-osteoporotic Fx	Up-regulated	No data available		
miR-124a	Seeliger et al.	Osteoporotic Fx vs non-osteoporotic Fx	Up-regulated	Inhibits osteoclast differentiation via NFATc1	Lee et al. [29]	
miR-125b	Seeliger et al.	Osteoporotic Fx vs non-osteoporotic Fx	Up-regulated	Inhibits osteogenic differentiation	Mizuno et al. [30]	
miR-133b	This study	Low trauma fracture vs control	Down-regulated ^a	Inhibits osteogenic differentiation via Runx2	Li et al. [10]	
	Li et al.	Low BMD vs normal BMD	Up-regulated			
miR-148a-3p	Seeliger et al.	Osteoporotic Fx vs non-osteoporotic Fx	Up-regulated	Promotes osteoclast differentiation via MAFB	Cheng et al. [31]	✓
miR-21-5p	Seeliger et al.	Osteoporotic Fx vs non-osteoporotic Fx	Up-regulated	Promotes osteogenic differentiation and impairs adipogenic differentiation	Trohatou, et al. [32]	✓
	Li et al.	Low BMD vs normal BMD	Down-regulated			
	This study	Low trauma fracture vs control	Up-regulated ^a			
miR-22-3p	This study	Low trauma fracture vs control	Down-regulated	Is up-regulated during osteogenic differentiation	Trompeter, et al. [9]	✓
miR-23a-3p	Seeliger et al.	Osteoporotic Fx vs non-osteoporotic Fx	Up-regulated	Inhibits osteogenic differentiation via SATB2	Hassan, et al. [33]	
miR-24-3p	Seeliger et al.	Osteoporotic Fx vs non-osteoporotic Fx	Up-regulated	Inhibits osteogenic differentiation via SATB2	Hassan, et al. [33]	✓
miR-328-3p	This study	Low trauma fracture vs control	Down-regulated	No data available		✓
miR-93-5p	Seeliger et al.	Osteoporotic Fx vs non-osteoporotic Fx	Up-regulated	Attenuates osteoblast mineralization	Yang, et al. [34]	

Fx, fracture; BMD, bone mineral density.

^a Regulation observed but not validated.

selected miRNAs (miR-21-5p, miR-146a-5p, miR-133b) in 120 post-menopausal women without fracture to normal, osteopenic or osteoporotic bone mineral density.

Based on an extended literature search, we found that the majority of circulating miRNAs had been previously characterized in vitro for their effects on bone formation and resorption, with the exception of miR-328-3p and miR-122. We selected 8 miRNAs from this list (Table 3), which were either not characterized at this point (miR-328-3p), only described in the context of osteoclast formation (miR-148a-3p) or transcriptomic analyses (miR-10b-5p, miR-22-3p), or chosen randomly from the list of known modulators of osteogenesis as controls (let-7 g-5p, miR-100-5p, miR-21-5p, miR-24-3p).

Seven miRNA mimics or inhibitors were transfected into adipose tissue-derived mesenchymal stem cells from two different female donors (HUF803 and HUF851), and tested for their effects on osteogenic differentiation using alkaline phosphatase (ALP) expression and cellular calcium deposition as relevant endpoints. Mesenchymal character of the ASCs was confirmed by flow cytometric analysis (see Supporting Fig. 5a) for the presence of MSC surface markers (C73 +, CD90 +, CD105 +) and absence of hematopoietic markers (CD14 –, CD34 –, CD45 –). In addition, the potential for osteogenic differentiation was confirmed by analysis of Runx2, Osteonectin, Osteocalcin, as well as ALP on day 7 after induction of osteogenic differentiation as well as calcium deposition by Alizarin Red staining after 21 days (Supporting Figs. 5b and c), albeit differences in the intensity of induction of these markers were observed depending on the donor.

The robustness as well as validity of the assay testing for the influence of miRNAs on osteogenic differentiation was confirmed by analyzing overexpression of hsa-miR-637, which was previously shown to impair proliferation and differentiation of hMSCs [26]. Indeed, transfection of miR-637 into ASCs resulted in significant miRNA overexpression (Figs. 3a/b) relative to a negative-control small RNA control. In consequence, reduced osteogenic differentiation in both primary ASC strains, as indicated by alkaline phosphatase activity on day 7 (Fig. 3c) and intracellular Ca²⁺ incorporation after 21 days were observed (Fig. 3d and Supporting Fig. 6 for representative images of Alizarin stainings).

Following the standard procedure developed for miR-637, qPCR analysis confirmed overexpression or knockdown of the selected miRNAs (Figs. 3a/b). The level of overexpression that could be achieved

was dependent on the endogenous expression level, which was lowest for miR-637 (highest overexpression) and highest for miR-21-5p (lowest overexpression). ALP and Ca²⁺ deposition data confirmed the previously published effects for miR-100-5p in both donors, whereas the effects of let-7g-5p, miR-21-5p and miR-24-3p were donor dependent. Overexpression of miR-148a-3p, which was previously described to promote osteoclast differentiation, also promoted osteogenic differentiation. From the candidates that were derived from this study and had not previously been studied, miR-10b-5p significantly impaired ALP activity and reduced Ca²⁺ deposition after 21 days compared to the control. The effects observed for miR-22-3p were not consistent between donors and miR-328-3p knockdown reduced the activity of ALP significantly, but not Ca²⁺ deposition.

Discussion

Several studies have shown that specific patterns of circulating miRNAs in plasma or serum correlate to the presence and progression of pathological conditions [13,35]. In this study we set out to compare the levels of secreted miRNAs in post-menopausal women suffering from recent osteoporotic femoral neck fractures to gender- and age-matched controls. This was done based on the hypothesis that the recent nature of fractures (<2 weeks prior to sampling) is likely to be reflected in the serum levels of mature miRNAs, and might be a response that is relevant to bone healing, specifically to bone formation. The exploratory analysis of 175 miRNAs identified several up- or down-regulated miRNAs in patients suffering from recent osteoporotic fractures. The list of differentially expressed miRNAs included miR-10a-5p, miR-10b-5p, miR-133b, miR-22-3p, miR-328-3p, and let-7g-5p, of which the latter three were confirmed in an independent set of samples as a validation cohort, despite the relatively small sample size.

Limitations of the study

The fact that the serum level changes of miR-10a/b and miR-133b could not be confirmed in the validation cohort might be a consequence of the low sample size, which often presents limitations in exploratory studies, as well as differences in clinical parameters between the cohorts. In the case of this study, the mean age of patients recruited for

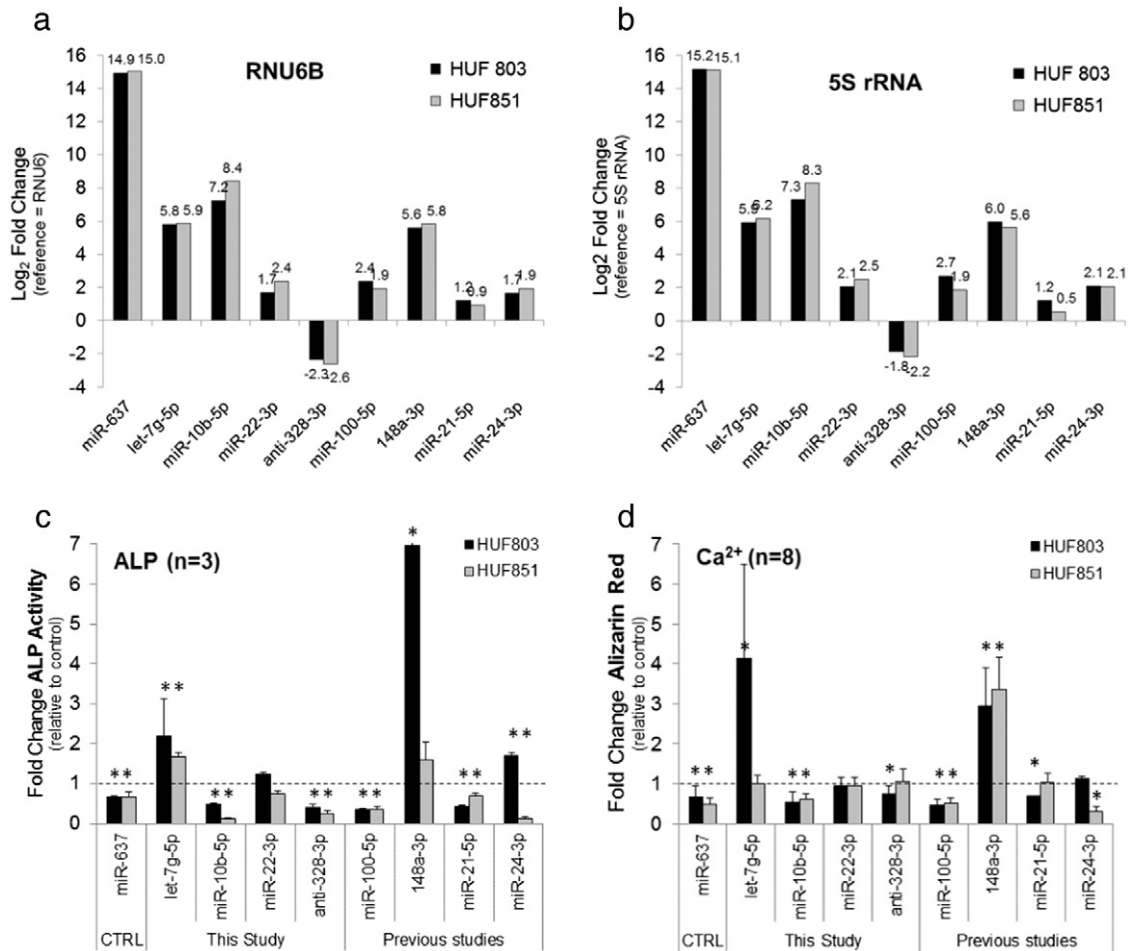


Fig. 3. In vitro transfection of miRNA mimics or inhibitors. Adipose tissue-derived stem cells (ASCs) from two female donors (HUF803 and HUF851) were transfected with mimics of miR-637 as positive control (637), miR-10b-5p (10b), miR-21-5p (21), miR-22-3p (22), miR-24-3p (24), miR-100-5p (100), miR-148a-3p (148a) or inhibitor against miR-328-3p (a-328). For control purposes, a non-targeting RNA control (NC) was transfected, and successful miRNA overexpression or knockdown was monitored by qPCR using RNU6 (a) or 5S rRNA (b) as reference genes. (c) Alkaline phosphatase (ALP) activity was assayed ($n = 3$) on day 7. Linear fold changes compared to negative control transfections are shown. (d) Mineralization of transfected ASCs was evaluated by Alizarin Red staining 21 days after differentiation ($n = 7$). Linear fold changes compared to negative control transfections are shown. Dotted lines indicate the reference level (fold change = 1). Data are presented as mean fold change \pm SD compared to control transfected cells ($n = 3$ for ALP, $n = 8$ for Alizarin Red staining). Statistical significance determined using the Holm-Sidak method, with $\alpha = 5.000\%$ indicated by an asterisk (*).

the discovery and validation study (71 years and 80 years, respectively) presents a second limitation. It has previously been reported that expression of certain miRNAs is altered during cellular senescence and aging [36,37]. One of the most prominent circulating miRNAs in the context of aging is miR-21-5p [14]. Indeed, although the levels of miR-21-5p did not change in response to recent osteoporotic fractures, it was significantly induced in the validation cohort compared to the discovery cohort, which might be related to elevated age and/or inflammation (Supporting Fig. 7). Further evaluation of current literature showed that miR-10a is also modulated in aging and inflammation of the endothelium in vitro and in vivo, which may significantly influence miR-10a serum levels [38,39]. For miR-22-3p, for which a stronger down-regulation in the validation group than in the discovery group was observed, an up-regulation during cellular senescence has been observed in human dermal fibroblasts, renal proximal tubular epithelial cells and CD8 + T-cell population [36]. As a consequence, it cannot be excluded that age-dependent effects might have limited the reproducibility of the discovery data in the validation cohort.

Besides age differences between the discovery and validation cohort, which might have compromised the validation results, also technical bias cannot be entirely excluded as source of variation. For the discovery study, global mean normalization was performed since this value was identified to show least variance across all samples [24]. For the

validation study, however, the approach of selecting a stable reference value was not possible, due to the low number of analyzed genes and the lack of robust reference miRNA for serum analysis. Consequently, data were processed using the results from spike-in controls to adjust for technical bias. This difference in normalization strategy might influence correlations between the discovery and validation data.

In general, blood-circulating miRNAs represent a complex readout of the physiological or pathophysiological processes in an organism. An interpretation of observed changes in circulating miRNAs is often difficult, since the majority of circulating miRNAs is expressed ubiquitously and cannot be precisely matched to a certain tissue. However, tissue-specific miRNAs have been identified [40,41] and shown to contain valuable information about localized aberrant tissue functions and proposed as novel markers of organ toxicity [42]. In the case of the miRNAs reported in this study, let-7g-5p, miR-10a/b and miR-22-3p are ubiquitously expressed, thus, it is not clear whether the changes reported in this study are due to aberrant expression in bone tissue. However, miR-133b was previously reported to be highly enriched in skeletal and heart muscle tissue [43], while miR-328 is enriched in brain tissue [44]. In addition, some of the here identified miRNAs also impact osteogenic differentiation, a sign that they might be causally related to processes that occurred at the time of blood sampling at around 2 weeks after fracture, such processes including bone healing.

Circulating miRNAs in patients with osteoporotic fractures might contribute to the molecular control of bone formation and resorption

Many of the here identified miRNAs have a ‘track record’ in the context of bone metabolism: miR-10b-5p and miR-22-3p were recently described by Trompeter et al. to be up-regulated in “unrestricted somatic stem cells” (USSC) on day 7 during osteogenic differentiation [9]. The authors also reported data from target validation experiments of genes that are relevant to osteogenic differentiation using luciferase 3' UTR reporter assays: overexpression of miR-10a-5p results in the down-regulation of CTNBP1, a negative regulator of WNT. Overexpression of miR-22-3p inhibited CDK6, an antagonist of BMP-2 signaling. Also Eguchi et al. report in their recent work data from a detailed characterization of miRNA transcription in mesenchymal stem cells undergoing osteogenic differentiation [45]. In contrast to Trompeter et al., they observed a down-regulation of miR-10b-5p and miR-22-3p during the differentiation, and consequently ascribed both miRNAs a role as stemness marker or negative modulator of osteogenic differentiation. This observation was confirmed in our experimental setting for miR-10b-5p. However, such controversies in data clearly demonstrate that miRNA function is highly cell type specific, as their activity strongly depends on the host cell transcriptome. In addition, donor dependent effects of miRNAs on osteogenic differentiation might be relevant. This can for example be caused by polymorphisms in miRNA binding sites, as shown by Lei et al. in the case of FGF-2 [46]. Also in the case of CDK6 several 3' UTR single-nucleotide polymorphisms have been reported [47], which remain to be studied in the context of miRNA binding sites.

Although the down-regulation of miR-133b in serum of fracture patients could not be confirmed during validation, expression levels of this miRNA in monocytes has been previously described as potential marker for bone disorders [48]. As part of the miR-206–miR-133b cluster, the skeletal muscle specific expression of this miRNA [40] and its importance for muscular tissue development has been well established [49]. Reduced serum levels of miR-133b might correlate with a loss in muscle tissue activity, which, however, might only be observed in specific fracture patients but not all. This could explain why levels of circulating miR-133b did not reach significance during validation.

Transcription of miR-328-3p is found in many human tissues and has been shown to become de-regulated in different types of cancer [50], potentially affecting WNT-signaling via repression of the WNT-inhibitor SFRP-1 [51]. Recently, it was shown that miR-328 targets the expression of CD44 in macrophages [52]. CD44 is also expressed in bone, especially high in osteocytes [53], where it helps extracellular binding to collagen. Here we show that the repression of miR-328-3p in ASCs significantly reduced ALP activity during osteogenic differentiation but did not affect calcium deposition.

Finally, the down-regulation of hsa-let-7g-5p is of interest, since the let-7 family of miRNAs is generally known to be almost silent in stem cells or progenitor cells, and to increase with cell differentiation in almost any type of somatic cell [54]. Indeed, it was reported that let-7 levels are increased during osteogenic lineage commitment of mesenchymal stem cells [55], and that ectopic expression of let-7 enhances osteoblast formation in vitro and in vivo by targeting HMGA2 [27]. Our in vitro data confirmed these effects in both donors on the level of ALP expression and in one donor on the level of Alizarin staining.

In summary, this study has expanded the knowledge of circulating miRNAs in the context of osteoporosis and osteoporotic fractures. For the majority of circulating miRNAs that responded to fractures, a link to specific functions in bone metabolism was found, or established as part of in vitro experiments in this study. This underlines the robustness of these results and indicates that these miRNAs might well be studied for their therapeutic activity in animal models of osteoporosis. In addition, once the detailed mechanisms of their mode-of-action have been established, the analysis of these circulating miRNAs could complement existing bone turnover markers currently used within clinical studies to

“measure” bone metabolism, bone healing, or efficacy of anti-osteoporotic treatments [56].

However, in order to define a concise clinical value of circulating miRNAs for the management of bone diseases, it is essential to analyze circulating miRNAs at baseline of prospective studies with fractures as end-points, or alternatively to study sample collectives from non-recent osteoporotic fractures to characterize a high-risk population but without detecting immediate consequences of bone regeneration. These prospective and retrospective studies will give insights into whether specific miRNAs signatures might also be helpful in improving current strategies for osteoporotic patient stratification according to their fracture risk [57].

Acknowledgments

This work was supported by the Christian Doppler Gesellschaft, Herzfelder'sche Familienstiftung, EU-FP7 Health Project FRAILOMIC 305483, EU-FP7 Health Project SYBIL 602300, FFG Femtech Grant 2013, and the Exiqon Grant Program 2013.

Authors roles

Study design: MH, PD, PP, RG and JG. Study conduct: MH, SW, SS, BS, MW, and VK. Data analysis: MH and SW. Data interpretation: MH, SW, PD, PP, RG and JG. Drafting manuscript: MH and SW. Revising manuscript content: MH, SW, PD, PP and JG. Approving final version of the manuscript: SW, PD, PP, JG and MH. MH takes responsibility for the integrity of data analysis.

Conflicts of interest

Dr. Matthias Hackl is employed by TAmiRNA GmbH. Johannes Grillari is the scientific-advisor of TAmiRNA and CSO of Evercyte GmbH.

Appendix A. Supplementary data

Supplementary data to this article can be found online at <http://dx.doi.org/10.1016/j.bone.2015.05.027>.

References

- [1] Kanis JA, McCloskey EV, Johansson H, Cooper C, Rizzoli R, Reginster J-Y, et al. European guidance for the diagnosis and management of osteoporosis in postmenopausal women. *Osteoporos Int* 2013;24:23–57. <http://dx.doi.org/10.1007/s00198-012-2074-y>.
- [2] Hernlund E, Svedbom A, Ivergård M, Compston J, Cooper C, Stenmark J, et al. Osteoporosis in the European Union: medical management, epidemiology and economic burden. A report prepared in collaboration with the International Osteoporosis Foundation (IOF) and the European Federation of Pharmaceutical Industry Associations (EFPIA). *Arch Osteoporos* 2013;8:136. <http://dx.doi.org/10.1007/s11657-013-0136-1>.
- [3] Cooper C, Harvey NC. Osteoporosis risk assessment. 2012;4191:1–2. <http://dx.doi.org/10.1136/bmj.e4191>.
- [4] Harvey N, Dennison E, Cooper C. Osteoporosis: impact on health and economics. *Nat Rev Rheumatol* 2010;6:99–105. <http://dx.doi.org/10.1038/nrrheum.2009.260>.
- [5] Bartel DP. MicroRNAs: target recognition and regulatory functions. *Cell* 2009;136:215–33. <http://dx.doi.org/10.1016/j.cell.2009.01.002>.
- [6] Dong S, Yang B, Guo H, Kang F. MicroRNAs regulate osteogenesis and chondrogenesis. *Biochem Biophys Res Commun* 2012;418:587–91. <http://dx.doi.org/10.1016/j.bbrc.2012.01.075>.
- [7] Zhao X, Xu D, Li Y, Zhang J, Liu T, Ji Y, et al. MicroRNAs regulate bone metabolism. *J Bone Miner Metab* 2013. <http://dx.doi.org/10.1007/s00774-013-0537-7>.
- [8] Van Wijnen AJ, van de Peppel J, van Leeuwen JP, Lian JB, Stein GS, Westendorf JJ, et al. MicroRNA functions in osteogenesis and dysfunctions in osteoporosis. *Curr Osteoporos Rep* 2013;11:72–82. <http://dx.doi.org/10.1007/s11914-013-0143-6>.
- [9] Trompeter H-I, Dreesen J, Hermann E, Iwaniuk KM, Hafner M, Renwick N, et al. MicroRNAs miR-26a, miR-26b, and miR-29b accelerate osteogenic differentiation of unrestricted somatic stem cells from human cord blood. *BMC Genomics* 2013;14:111. <http://dx.doi.org/10.1186/1471-2164-14-111>.
- [10] Li Z, Hassan MQ, Volinia S, van Wijnen AJ, Stein JL, Croce CM, et al. A microRNA signature for a BMP2-induced osteoblast lineage commitment program. *Proc Natl Acad Sci U S A* 2008;105:13906–11. <http://dx.doi.org/10.1073/pnas.0804438105>.
- [11] Kapinas K, Kessler CB, Delany AM. miR-29 suppression of osteonectin in osteoblasts: regulation during differentiation and by canonical Wnt signaling. *J Cell Biochem* 2009;108:216–24. <http://dx.doi.org/10.1002/jcb.22243>.

- [12] Mizoguchi F, Izu Y, Hayata T, Hemmi H, Nakashima K, Nakamura T, et al. Osteoclast-specific Dicer gene deficiency suppresses osteoclastic bone resorption. *J Cell Biochem* 2010;109:866–75. <http://dx.doi.org/10.1002/jcb.22228>.
- [13] Weilner S, Schraml E, Redl H, Grillari-Voglauer R, Grillari J. Secretion of microvesicular miRNAs in cellular and organismal aging. *Exp Gerontol* 2013;48:626–33. <http://dx.doi.org/10.1016/j.exger.2012.11.017>.
- [14] Olivieri F, Spazzafumo L, Santini G, Lazzarini R, Albertini MC, Rippon MR, et al. Age-related differences in the expression of circulating microRNAs: miR-21 as a new circulating marker of inflammation. *Mech Ageing Dev* 2012;133:675–85. <http://dx.doi.org/10.1016/j.mad.2012.09.004>.
- [15] Seeliger C, Karpinski K, Haug AT, Vester H, Schmitt A, Bauer JS, et al. Five freely circulating miRNAs and bone tissue miRNAs are associated with osteoporotic fractures. *J Bone Miner Res* 2014;29:1718–28. <http://dx.doi.org/10.1002/jbmr.2175>.
- [16] Li H, Wang Z, Fu Q, Zhang J. Plasma miRNA levels correlate with sensitivity to bone mineral density in postmenopausal osteoporosis patients. *Biomarkers* 2014;19:553–6. <http://dx.doi.org/10.3109/1354750X.2014.935957>.
- [17] Ismail N, Wang Y, Dakhlallah D, Moldovan L, Agarwal K, Batte K, et al. Macrophage microvesicles induce macrophage differentiation and miR-223 transfer. *Blood* 2013;121:984–95. <http://dx.doi.org/10.1182/blood-2011-08-374793>.
- [18] Zhu H, Fan G-C. Extracellular/circulating microRNAs and their potential role in cardiovascular disease. *Am J Cardiovasc Dis* 2011;1:138–49.
- [19] Canalis E. Wnt signalling in osteoporosis: mechanisms and novel therapeutic approaches. *Nat Rev Endocrinol* 2013;9:575–83. <http://dx.doi.org/10.1038/nrendo.2013.154>.
- [20] Asagiri M, Takayanagi H. The molecular understanding of osteoclast differentiation. *Bone* 2007;40:251–64. <http://dx.doi.org/10.1016/j.bone.2006.09.023>.
- [21] Wolbank S, Ph D, Stadler G, Peterbauer A, Sc M, Katinger H, et al. Telomerase immortalized human amnion- and adipose-derived mesenchymal stem cells: maintenance of differentiation and immunomodulatory characteristics. *Tissue Eng Part A* 2009;15:1843–54. <http://dx.doi.org/10.1089/ten.tea.2008.0205.Telomerase>.
- [22] Blondal T, Jensby Nielsen S, Baker A, Andreassen D, Mouritzen P, Wrang Teilmum M, et al. Assessing sample and miRNA profile quality in serum and plasma or other biofluids. *Methods* 2013;59:S1–6. <http://dx.doi.org/10.1016/j.jmeth.2012.09.015>.
- [23] Reynoso R, Laufer N, Hackl M, Skalicky S, Monteforte R, Turk G, et al. MicroRNAs differentially present in the plasma of HIV elite controllers reduce HIV infection in vitro. *Sci Rep* 2014;4:5915. <http://dx.doi.org/10.1038/srep05915>.
- [24] Andersen CL, Jensen JL, Ørntoft TF. Normalization of real-time quantitative reverse transcription-PCR data: a model-based variance estimation approach to identify genes suited for normalization, applied to bladder and colon cancer data sets. *Cancer Res* 2004;64:5245–50. <http://dx.doi.org/10.1158/0008-5472.CAN-04-0496>.
- [25] Sanders R, Mason DJ, Foy CA, Huggert JF. Considerations for accurate gene expression measurement by reverse transcription quantitative PCR when analysing clinical samples. *Anal Bioanal Chem* 2014. <http://dx.doi.org/10.1007/s00216-014-7857-x>.
- [26] Zhang J, Fu W, He M, Wang H, Wang W, Yu S, et al. MiR-637 maintains the balance between adipocytes and osteoblasts by directly targeting Osterix. *Mol Biol Cell* 2011;22:3955–61. <http://dx.doi.org/10.1091/mbc.E11-04-0356>.
- [27] Wei J, Li H, Wang S, Li T, Fan J, Liang X, et al. let-7 enhances osteogenesis and bone formation while repressing adipogenesis of human stromal/mesenchymal stem cells by regulating HMGA2. *Stem Cells Dev* 2014;23:1452–63. <http://dx.doi.org/10.1089/scd.2013.0600>.
- [28] Zeng Y, Qu X, Li H, Huang S, Wang S, Xu Q, et al. MicroRNA-100 regulates osteogenic differentiation of human adipose-derived mesenchymal stem cells by targeting BMP2. *FEBS Lett* 2012;586:2375–81. <http://dx.doi.org/10.1016/j.febslet.2012.05.049>.
- [29] Lee Y, Kim HJ, Park CK, Kim Y-G, Lee H-J, Kim J-Y, et al. MicroRNA-124 regulates osteoclast differentiation. *Bone* 2013;56:383–9. <http://dx.doi.org/10.1016/j.bone.2013.07.007>.
- [30] Mizuno Y, Yagi K, Tokuzawa Y, Kanesaki-Yatsuka Y, Suda T, Katagiri T, et al. miR-125b inhibits osteoblastic differentiation by down-regulation of cell proliferation. *Biochem Biophys Res Commun* 2008;368:267–72. <http://dx.doi.org/10.1016/j.bbrc.2008.01.073>.
- [31] Cheng P, Chen C, He H-B, Hu R, Zhou H-D, Xie H, et al. miR-148a regulates osteoclastogenesis by targeting V-maf musculoaponeurotic fibrosarcoma oncogene homolog B. *J Bone Miner Res* 2013;28:1180–90. <http://dx.doi.org/10.1002/jbmr.1845>.
- [32] Trohatou O, Zagoura D, Bitsika V, Pappa KI, Antsaklis A, Anagnostou NP, et al. Sox2 suppression by miR-21 governs human mesenchymal stem cell properties. *Stem Cells Transl Med* 2014;3:54–68. <http://dx.doi.org/10.5966/sctm.2013-0081>.
- [33] Hassan MQ, Gordon JAR, Belotti MM, Croce CM, van Wijnen AJ, Stein JL, et al. A network connecting Runx2, SATB2, and the miR-23a ~ 27a ~ 24-2 cluster regulates the osteoblast differentiation program. *Proc Natl Acad Sci U S A* 2010;107:19879–84. <http://dx.doi.org/10.1073/pnas.1007698107>.
- [34] Yang L, Cheng P, Chen C, He H-B, Xie G-Q, Zhou H-D, et al. miR-93/Sp7 function loop mediates osteoblast mineralization. *J Bone Miner Res* 2012;27:1598–606. <http://dx.doi.org/10.1002/jbmr.1621>.
- [35] De Guire V, Robitaille R, Tétreault N, Guérin R, Ménard C, Bambace N, et al. Circulating miRNAs as sensitive and specific biomarkers for the diagnosis and monitoring of human diseases: promises and challenges. *Clin Biochem* 2013;46:846–60. <http://dx.doi.org/10.1016/j.clinbiochem.2013.03.015>.
- [36] Hackl M, Brunner S, Fortschegger K, Schreiner C, Micutkova L, Mück C, et al. miR-17, miR-19b, miR-20a, and miR-106a are down-regulated in human aging. *Aging Cell* 2010;9:291–6. <http://dx.doi.org/10.1111/j.1474-9726.2010.00549.x>.
- [37] Grillari J, Hackl M, Grillari-Voglauer R. miR-17-92 cluster: ups and downs in cancer and aging. *Biogerontology* 2010;11:501–6.
- [38] Qin B, Yang H, Xiao B. Role of microRNAs in endothelial inflammation and senescence. *Mol Biol Rep* 2012;39:4509–18. <http://dx.doi.org/10.1007/s11033-011-1241-0>.
- [39] Fang Y, Shi C, Manduchi E, Civelek M, Davies PF. MicroRNA-10a regulation of proinflammatory phenotype in athero-susceptible endothelium in vivo and in vitro. *Proc Natl Acad Sci U S A* 2010;107:13450–5. <http://dx.doi.org/10.1073/pnas.1002120107>.
- [40] McCarthy JJ. MicroRNA-206: the skeletal muscle-specific myomiR. *Biochim Biophys Acta* 2008;1779:682–91. <http://dx.doi.org/10.1016/j.bbagr.2008.03.001>.
- [41] Lin Q, Wei W, Coelho CM, Li X, Baker-Andersen D, Dudley K, et al. The brain-specific microRNA miR-128b regulates the formation of fear-extinction memory. *Nat Neurosci* 2011;14:1115–7. <http://dx.doi.org/10.1038/nn.2891>.
- [42] Mikaelian I, Scicchitano M, Mendes O, Thomas RA, LeRoy BE. Frontiers in preclinical safety biomarkers: microRNAs and messenger RNAs. *Toxicol Pathol* 2012;18–31. <http://dx.doi.org/10.1177/0192623312448939>.
- [43] Zaharieva IT, Calissano M, Scoto M, Preston M, Cirak S, Feng L, et al. Dystromirs as serum biomarkers for monitoring the disease severity in duchenne muscular dystrophy. *PLoS ONE* 2013;8:e80263. <http://dx.doi.org/10.1371/journal.pone.0080263>.
- [44] Liang Y, Ridzon D, Wong L, Chen C. Characterization of microRNA expression profiles in normal human tissues. *BMC Genomics* 2007;8:166. <http://dx.doi.org/10.1186/1471-2164-8-166>.
- [45] Eguchi T, Watanabe K, Hara ES, Ono M, Kuboki T, Calderwood SK. OsteomiR: a novel panel of microRNA biomarkers in osteoblastic and osteocytic differentiation from mesenchymal stem cells. *PLoS ONE* 2013;8:e58796. <http://dx.doi.org/10.1371/journal.pone.0058796>.
- [46] Lei S-F, Pappasian CJ, Deng H-W. Polymorphisms in predicted miRNA binding sites and osteoporosis. *J Bone Miner Res* 2011;26:72–8. <http://dx.doi.org/10.1002/jbmr.186>.
- [47] Traganavante V, Barnes MR, Ganesh SK, Lanktree MB, Guo W, Franceschini N, et al. Gene-centric meta-analysis in 87,736 individuals of European ancestry identifies multiple blood-pressure-related loci. *Am J Hum Genet* 2014;94:349–60. <http://dx.doi.org/10.1016/j.ajhg.2013.12.016>.
- [48] Wang Y, Li L, Moore BT, Peng X-H, Fang X, Lappe JM, et al. MiR-133a in human circulating monocytes: a potential biomarker associated with postmenopausal osteoporosis. *PLoS ONE* 2012;7:e34641. <http://dx.doi.org/10.1371/journal.pone.0034641>.
- [49] Kornfeld J-W, Brüning JC. MyomiRs-133a/b turn off the heat. *Nat Cell Biol* 2012;14:1248–9. <http://dx.doi.org/10.1038/ncb2642>.
- [50] Tokarz P, Blasiak J. The role of microRNA in metastatic colorectal cancer and its significance in cancer prognosis and treatment. *Acta Biochim Pol* 2012;59:467–74.
- [51] Delic S, Lottmann N, Stelzl A, Liesenberg F, Wolter M, Götze S, et al. MiR-328 promotes glioma cell invasion via SFRP1-dependent Wnt-signaling activation. *Neuro Oncol* 2014;16:179–90. <http://dx.doi.org/10.1093/neuonc/not164>.
- [52] Ishimoto T, Sugihara H, Watanabe M, Sawayama H, Iwatsuki M, Baba Y, et al. Macrophage-derived reactive oxygen species suppress miR-328 targeting CD44 in cancer cells and promote redox adaptation. *Carcinogenesis* 2014;35:1003–11. <http://dx.doi.org/10.1093/carcin/bgt402>.
- [53] Hughes DE, Salter DM, Simpson R. CD44 expression in human bone: a novel marker of osteocytic differentiation. *J Bone Miner Res* 1994;9:39–44. <http://dx.doi.org/10.1002/jbmr.5650090106>.
- [54] Boyerinas B, Park S-M, Hau A, Murmann AE, Peter ME. The role of let-7 in cell differentiation and cancer. *Endocr Relat Cancer* 2010;17:F19–36. <http://dx.doi.org/10.1677/ERC-09-0184>.
- [55] Bakhshandeh B, Soleimani M, Hafizi M, Paylakhi SH, Ghaemi N. MicroRNA signature associated with osteogenic lineage commitment. *Mol Biol Rep* 2012;39:7569–81. <http://dx.doi.org/10.1007/s11033-012-1591-2>.
- [56] Garner P. New developments in biological markers of bone metabolism in osteoporosis. *Bone* 2014;66:46–55. <http://dx.doi.org/10.1016/j.bone.2014.05.016>.
- [57] Huang J, Chen D. miRNAs in circulation: mirroring bone conditions? *J Bone Miner Res* 2014;29:1718–28. <http://dx.doi.org/10.1002/jbmr.2297>.